GDCh Research Article Angewandte International Edition Chemie www.angewandte.org

How to cite: *Angew. Chem. Int. Ed.* **2025**, *64*, e202502474
doi.org/10.1002/anie.202502474

Sustainable Chemistry

Room-Temperature Material Recycling/Upcycling of Polyamide Waste Enabled by Cosolvent-Tunable Dissolution Kinetics

Jonathon Tanks and Kenji Tamura**

Abstract: Polyamides (PAs, nylons) are a ubiquitous class of high-performance plastics used extensively in a wide range of applications. Their high resistance to many common solvents and tendency to hydrolyze in strong acids or bases creates a major hurdle to low-emissions material recycling (i.e., resource separation and recovery). In the present study, the first detailed investigation into the molecular mechanisms of polyamide dissolution, we show that introducing a weakly hydrogen-bonding cosolvent into formic acid can effectively tune the solvent–solvent and solvent–polymer interactions, drastically accelerates the room-temperature dissolution kinetics of common (short-chain) polyamides such as PA6 and PA66, as well as long-chain and semi-aromatic varieties. The recovered polymers show no change in their chemical structures or properties, and sufficient selectivity allows for fillers such as short and long fibers, inorganic nanoparticles, metals, and other mixed polymer phases to be recovered at high efficiency (>95%) along with recirculation of all solvents (>98%). This cosolvent-enabled approach has the potential to make polyamide recycling more sustainable and economical by reducing the energy input and CO_2 emissions required to separate and recover the various constituent materials from automotive and electrical components, textiles, and beyond.

Introduction

Polyamides (PAs, or nylon) exhibit excellent heat resistance and mechanical properties, making them a key material in numerous industries ranging from automotive, electrical/electronics, textiles, and fishing/leisure and represent a market size of 8 Mt yr^{-1} valued at 40 bil \$ yr^{-1} (Figure 1a).[1,2] The synthesis of conventional polyamides such as PA6 and PA66 uses non-renewable feedstocks and carries a large carbon footprint (6-9 kg CO_2-eq kg^{-1}) energy demand (35–60 MJ kg^{-1}).[3,4] Recycling technology for PAs has received far less attention than other plastics, e.g., PET, despite their high cost and widespread use. As a result, polyamides often end up in landfills and even the ocean.[1,3,5]

PAs are commonly used in blends and composites containing secondary materials (SM) such as fibers/microparticles, metals, and polyesters, some of which are high-value or carry a large carbon footprint and should be recovered for both resource circularity and carbon neutrality (Figure 1a). Chemical recycling (de-/re-polymerization) can regenerate a high-quality product (i.e., large contribution to resource circularity), but it is a fundamentally high-temperature process (180–300 °C) with high energy demand for both the depolymerization and repolymerization steps (i.e., small contribution to carbon neutrality).[1,6–10] Some promising strategies for chemical recycling under milder conditions include the synthesis of novel lactam monomers with lower ring strain energy or catalyzed conversion of commercial PAs into tertiary amine-based value-added chemicals,[11,12] but these approaches still have the downsides of relatively low yield (40%–85%) and high energy demand (>180 °C, >15 hr). By contrast, mechanical recycling (grinding/extrusion) is technologically simple and boasts the lowest carbon emissions of any plastic recycling method available, but separation of PAs from SMs is too difficult to make it impractical in many cases and the resulting materials often show degraded performance.[13–16]

Physical recycling (dissolution/precipitation) can selectively dissolve certain plastics and recover the target materials without complete deconstruction into monomers.[17–22] Patented processes like Creasolv[23,24] or STRAP[25,26] involve dissolving waste plastic products such as packaging films in a polymer-specific solvent system, by which constituent materials can then be separated and purified. The solvents are usually selected using Hansen solubility parameter (HSP) theory[27] or COSMO-RS[25,26,28,29] implicit solvation models, the former of which is a thermodynamic model of interactions expressed by cohesive energy density, and the latter of which is a molecular model of interactions expressed by surface

[*] Dr. J. Tanks
Research Center for Structural Materials, National Institute for Materials Science, 1-2-1 Sengen, Tsukuba 305-0047, Japan
E-mail: tanks.jonathon@nims.go.jp

Dr. K. Tamura
Research Center for Electronic and Optical Materials, National Institute for Materials Science, 1-1 Namiki, Tsukuba 305-0044, Japan
E-mail: tamura.kenji@nims.go.jp

Additional supporting information can be found online in the Supporting Information section

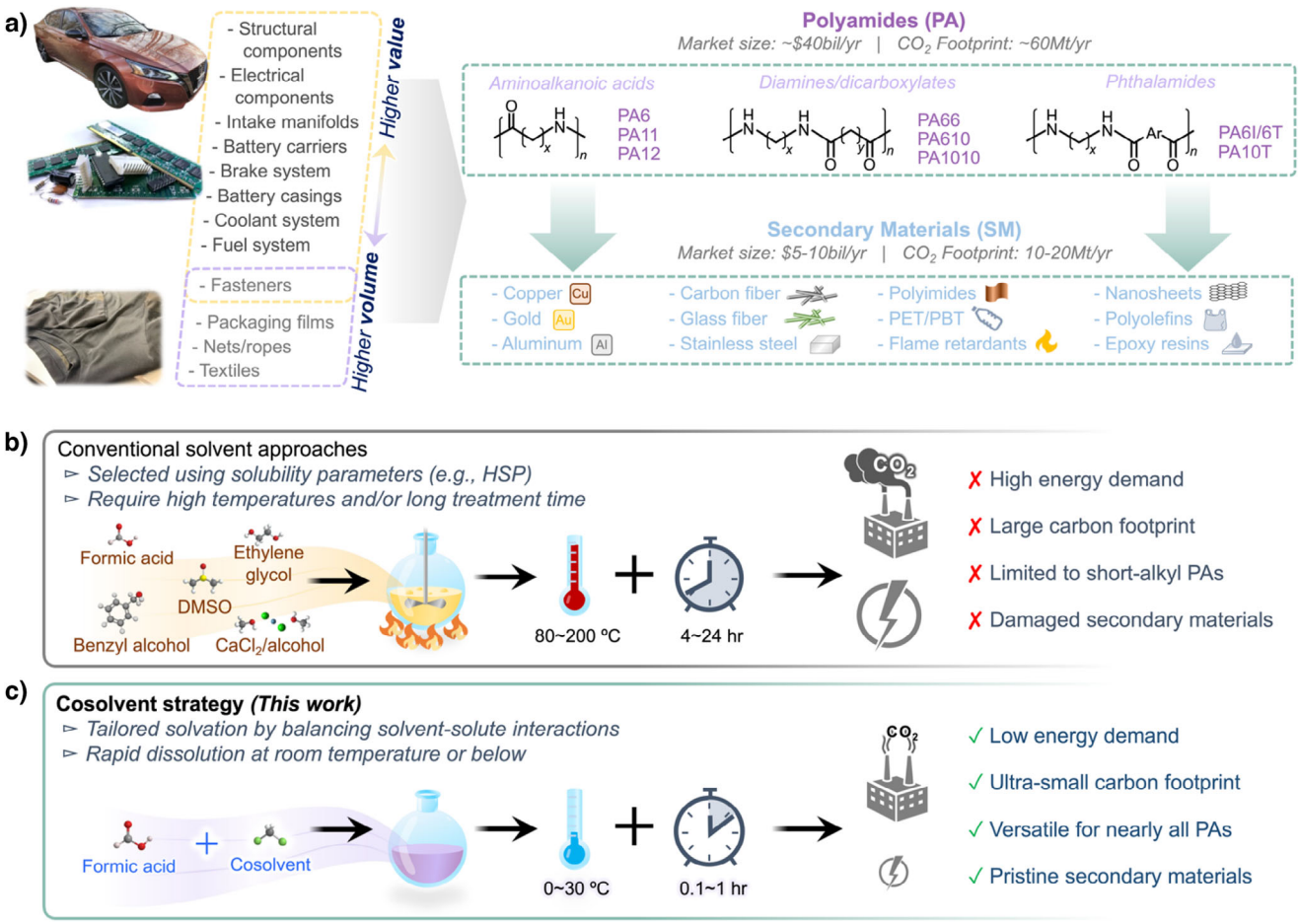

Figure 1. a) Polyamide (PA) components and products, ranging from structural/electrical composites to textiles. The high-value components typically contain polyamide mixed with valuable secondary materials. b) Conventional dissolution-based approaches involve solvent selection by solubility parameter (e.g., HSP) theory and require high temperatures and relatively long treatment times, resulting in high energy consumption and a large carbon footprint. c) This work demonstrates that a cosolvent strategy accelerates PA dissolution in formic acid at room temperature, resulting in an unprecedented reduction in energy consumption and overall carbon footprint.

charge distribution in response to a dielectric continuum. However, these techniques often fail to accurately reproduce interactions in strongly hydrogen-bonded organic molecules due to the complex nature of these systems compared to nonpolar and aprotic-polar systems.[28,29]

The majority of research studies and patented technologies regarding PA dissolution—mostly electrospinning, but some recycling—employ either formic acid (FA) or polar solvents (e.g., benzyl alcohol), which vary widely in their agreement with HSP predictions (Figure S1).[17–24] While FA can dissolve PA6 and other short-chain PAs at room temperature, the slow kinetics can make complete dissolution take up to 24 hr depending on the recyclate geometry. Other polar solvents require high temperatures (140 °C–200 °C) and long dissolution times (4–24 hr),[1,17–24] which is comparable to chemical recycling conditions in terms of carbon footprint (Figure 1b). Furthermore, long-chain PAs (e.g., PA12 and bio-based PA11) only dissolve in pure FA at elevated temperatures (−80 °C) and require long dissolution times (4–24 hr).[30,31] High-performance semi-aromatic polyphthalamides (PPAs) are even more resistant to these solvents and do not dissolve even under harsh conditions. By contrast, fluorinated alcohols and acids such as hexafluoroisopropanol (HFIP) and trifluoroacetic acid (TFA) can easily dissolve a range of PAs (short- and long-chain) at ambient conditions,[32] but they are too expensive to be used in an economically viable scaled-up recycling process. There is an urgent need for a versatile and cost-effective recycling method that can recover valuable resources from a range of polyamide-containing waste with minimal carbon emissions.[33–35]

In this work, we present the first (to the authors' knowledge) detailed elucidation of the molecular mechanisms of polyamide dissolution through a combination of experiments and density functional theory (DFT) calculations, and more specifically demonstrate that the addition of a weakly H-bonding cosolvent to formic acid (FA) drastically enhances the dissolution kinetics of polyamides without heat or agitation, resulting in complete dissolution in under 1 hr at room temperature. This novel cosolvent strategy can be used in a dissolution-based physical recycling process that is universal and rapid for any aliphatic-containing polyamide and can

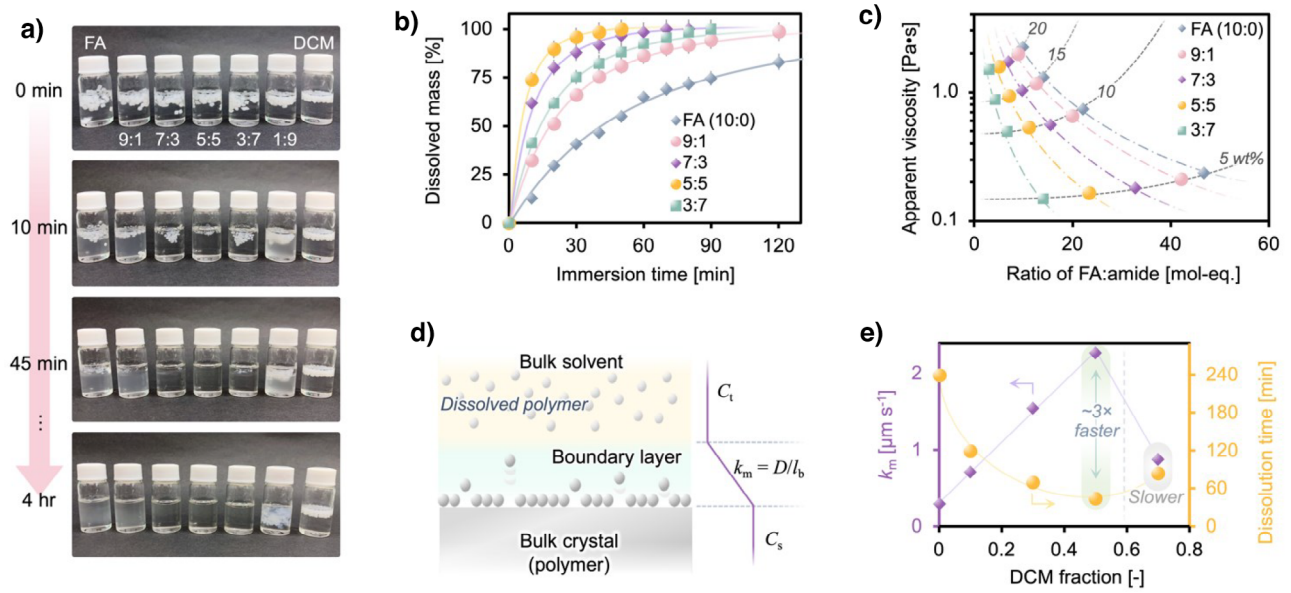

Figure 2. (a) Photographs and (b) mass change measurements of PA6 pellets dissolving at room temperature (no agitation) in formic acid (FA)-based cosolvent system with different cosolvent ratios (w/w). (c) Apparent viscosity of PA6 solutions with different solids concentrations and cosolvent fractions. (d) Schematic of the solid-liquid interface during crystal dissolution, where k_m is a measure of mass transfer across the boundary layer (thickness l_b) according to the Noyes-Whitney model. (e) Influence of cosolvent fraction on the mass transfer coefficient k_m and total dissolution time.

be performed at ambient conditions with very low energy consumption (Figure 1c). Application to a variety of different polyamides and fillers with high yield and quality demonstrates the merit of this approach toward separation and recovery of valuable resources such as carbon and glass fibers, metals, and nanofillers, in addition to all. Carbon footprint and economic cost were calculated to be substantially lower than other physical or chemical recycling methods.

Results and Discussion

Polyamide Dissolution in a Cosolvent System

It is well known that short-chain PAs dissolve in FA at room temperature (RT), but it can take up to 12 h for complete dissolution. As shown in Figure 2a, PA6 formed a slightly cloudy solution after 4 hr in pure FA (RT, no agitation), whereas PA66 became completely clear (Figure S2). After screening various solvents (see Supporting Information), a measurable positive effect on the dissolution rate of PA6 was only observed for chlorinated hydrocarbons like dichloromethane (DCM), chloroform ($CHCl_3$), and dichloroethane (DCE); they have characteristic low polarity and the ability to form weak H-bonds and effectively solvate hydrocarbons.[36] Ethyl acetate (EtOAc), MEK, and THF are similar to DCM in terms of, e.g. viscosity and HSPs, but they had the opposite effect of decreasing overall solubility. H-bond titration of PA6 solutions revealed that FA is more sensitive than PA to the cosolvent and that solubility shows strong negative correlation with the cosolvent's donor number (DN) (Figure S3). This means it must act as a weak H-bond donor (HBD) and poor H-bond acceptor (HBA) to promote polyamide dissolution. This characteristic has been demonstrated for fluorinated polar solvents such as HFIP,[37] suggesting that chlorinated hydrocarbons combined with formic acid can serve the same role.

DCM was selected as the primary cosolvent for our study due to its compatibility with FA, relatively low cost, and low boiling point. PAs do not dissolve in pure DCM at RT (Figure 2a), contrary to predictions by HSP theory and implicit solvation models which do not account for explicit H-bonding (Figure S1). PA6 dissolution in FA/DCM mixtures is accelerated by varying degrees depending on the cosolvent ratio, reaching a maximum at 1:1 w/w (i.e., DCM fraction of $f_{DCM} = 0.5$) and reversing to a slower rate at $f_{DCM} = 0.7$ (Figure 2b). When $f_{DCM} > 0.7$, only swelling with limited dissolution is observed. Viscosity measurements of PA6 solutions at different solids concentrations and cosolvent ratios, shown in Figure 2c normalized to the molar ratio of FA to amide units, made it clear that higher f_{DCM} correlates to lower solution viscosity with the lowest value obtained when $f_{DCM} = 0.7$, which tells us that dissolution rate is not necessarily affected by viscosity of the bulk solvent or solution (Figure S2).

Considering the polyamide as a semi-crystalline solid, the dissolution of the crystalline fraction would be the rate-limiting step. Employing the Brunner–Nernst model[38,39] to analyze the mass transfer process at the polymer-solvent interface (Figure 2d; details in Supporting Information), we found that the mass transfer coefficient (k_m) for PA through a boundary layer (L_b) between bulk crystal and bulk solvent increases linearly with cosolvent fraction up to $f_{DCM} = 0.5$ and then sharply decreases at $f_{DCM} = 0.7$ (Figure 2e), and

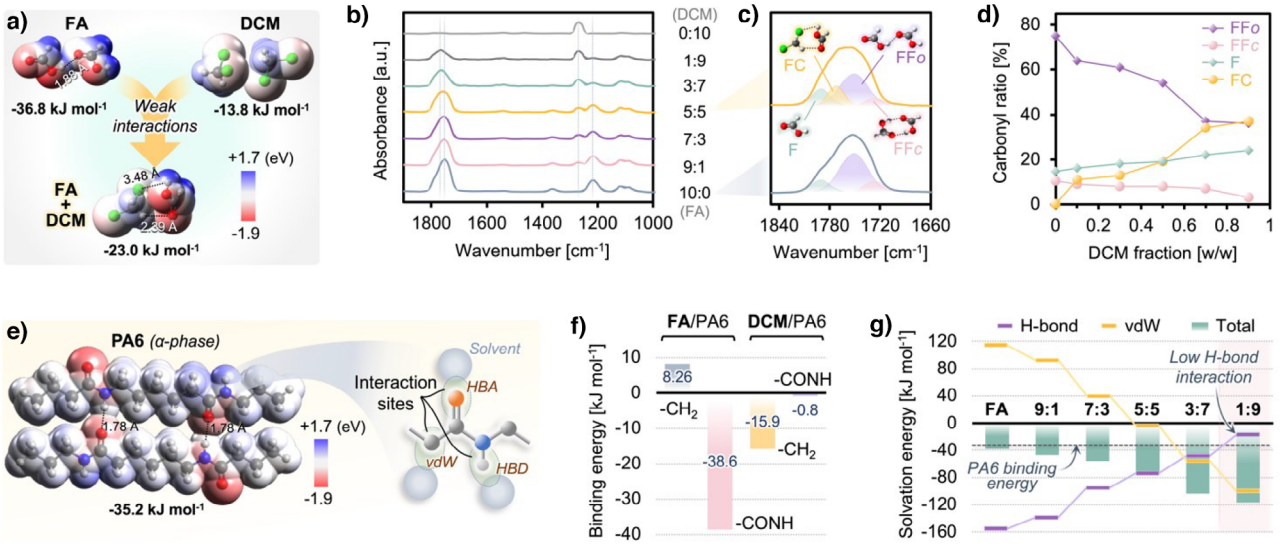

Figure 3. a) Molecular electrostatic potentials (MEP), binding energies (kJ/mol), and H-bond lengths (Å) for dimers of FA (FF), DCM (CC), and FA/DCM (FC). b) FTIR spectra of FA with different cosolvent fractions (f_{DCM}), and c) magnified carbonyl region with deconvoluted peaks for open (FF*o*) and closed (FF*c*) and monomer (F) forms of FA, and the FC dimer. (d) Changes in integrated areas of carbonyl bands representing each interaction shown in (c) for different cosolvent fractions. (e) Structure and MEP of H-bonded PA6 oligomer representing the α-phase crystal and schematic of solvent interaction sites. f) Approximate binding energies for FA and DCM at each binding site. g) Total solvation energy ΔG_{solv} and approximated H-bond and vdW components.

its independence of specific surface area suggests a surface erosion-type dissolution mechanism (Figure S4).

Cosolvent-Regulated Intermolecular Interactions

DFT calculations of binding energies (ΔE_{bind}) at the M06-2X/def2-TZVP level[40,41] for dimers of pure FA and DCM and FA/DCM are shown in Figure 3a (see Supporting Information for details). FA in bulk solvent form is assumed to consist primarily of so-called "open" dimers (FF*o*)[42–48] with moderately large ΔE_{bind} dominated by H-bonding, while the mildly polar DCM dimer has a smaller ΔE_{bind} dominated by van der Waals (vdW) interactions.[49–51] Combining them into the solvent-cosolvent dimer (FC) yields smaller ΔE_{bind} and longer H-bond lengths than pure FA (Figures 3a and S5), with FA and DCM acting as the HBA and HBD, respectively. FTIR spectroscopy of the cosolvent system revealed a blue-shift in the C=O region of FA with increasing f_{DCM} (Figures 3b–d) which was reproduced by DFT (Figure S5). We attribute this shift to the transition from FF clusters to FC and (albeit rare) F monomers.[42–51] These results imply the presence of weak hydrogen bonds between FA and DCM, with the largest shift occurring between $0.5 < f_{DCM} < 0.7$. Replacing DCM with EtOAc, which negatively affected PA6 solubility, gives a FC dimer with larger ΔE_{bind} than FF (Figure S5), supporting our assertion that weak H-bonds play a major role in dissolution kinetics. We next examined the solvent-polymer interactions using DFT and FTIR. The PA6 oligomer used in our DFT study is the α-phase crystal configuration (PA6-α)[52–54] depicted in Figure 3e, with possible solvent interaction sites identified as the amide group (-CONH) and methylene groups (-CH_2) that act through HBA/HBD or vdW-dominant interactions, respectively. The individual binding energies of FA and DCM monomers with PA6 at these sites are compared in Figure 3f. Figure 3g shows steady growth of the so-called solvation energy (ΔG_{solv}) of PA6-α, which we take as the binding energy between an explicit solvent cluster and polymer oligomers, with increasing cosolvent fraction up to $f_{DCM} = 0.9$ (see Supporting Information for details). Final solvated structures for $0 \leq f_{DCM} < 0.7$ show full breakage of H-bonds and conformational change of the alkyl segment, whereas H-bonds are partially and fully intact at $f_{DCM} = 0.7$ and 0.9, respectively (Figure S6). Using the binding energies of individual solvent-polymer interactions to decompose ΔG_{solv} into approximate H-bond and vdW components, we see that poor affinity of FA toward methylene units in PA6 results in a large endergonic vdW component, but the strong H-bond component is large enough to create a net exergonic interaction that exceeds the ΔE_{bind} of PA6-α; this explains why short-chain PAs dissolve in pure FA at room temperature. As f_{DCM} increases, the two components approach each other while the total ΔG_{solv} continues to grow larger until $f_{DCM} = 0.9$, at which point the H-bond component grows smaller than the pure PA6-α binding energy (Figure S7, Table S3).

Cosolvent Effect on Dissolution Kineticss

H-bonds within the polyamide crystal must be broken for dissolution to occur, which is only probable when the solvent-polymer interaction (i.e., ΔG_{solv}) has a sufficiently large H-bond component, specifically the HBD contribution. This explains why PAs do not dissolve in pure DCM or even FA/DCM at $f_{DCM} = 0.9$, whereas polycaprolactone (PCL)

readily dissolves in DCM despite only differing from PA6 by the amide/ester moiety.[55] In addition to the thermodynamic aspects of solubility, the dissolution kinetics must also be affected by the balance of H-bond and vdW contributions. Thus, two conditions for enhancing dissolution kinetics are 1) overcoming inter-chain attraction by vdW interactions with methylene units, and 2) ensuring preferential solvent-polymer interaction by tuning the solvent–solvent interactions.

In particular, polyamides are semi-crystalline polymers typically exhibiting a highly stable α-phase crystal formed by H-bonding; this must be overcome for decrystallization occur, followed by conventional dissolution mechanisms (i.e., disentanglement and diffusion).[56] DFT calculations of PA6-α (H-bonded oligomers) and solvated PA6 chains in explicit solvent clusters indicated that the N─H and C═O bonds do not significantly change when going from crystal to solution, as the corresponding HBA/HBD simply changes from PA to FA with similar binding energies (Figures 3 and S8). However, our calculations show that the carbonyl C─N (CONH) bond is sensitive to the HBA/HBD species, and experimental and theoretical studies have demonstrated that -CONH exhibits distinctly different IR absorption bands (850–1100 cm^{-1}) depending on the crystal structure.[52–54] By monitoring this band for a thin PA6 film exposed to FA/DCM (1:1 w/w) using transmission-mode FTIR, we found an exponential-type decrease over time that indicates rapid decrystallization in the early stages of solvent contact (Figure S8).

To explain the relationship between solution properties (i.e., viscosity, ΔG_{solv}, and D) and dissolution rate, we consider the conditions for dissolution listed above and hypothesize that thermodynamics may affect kinetics for polyamides in a way similar to inorganic and molecular crystals.[57–59] If a large (negative) value of total solvation energy ΔG_{solv} promotes solubility, and a minimum H-bond component is required to break H-bonds in the crystal, the dissolution process can be thought of as a competition between the mutual solvation of FA/cosolvent and the solvation of polyamide. The addition of weakly H-bonding cosolvent does two things: i) breaks up the FA network through weak-HBD/poor-HBA action, and ii) increases vdW interactions with the polyamide, both of which promote more favorable solvent–polymer interactions (Figure 4a).

The question becomes, at what point does the cosolvent negatively affect dissolution kinetics despite more favorable ΔG_{solv}? Considering the role of cosolvent described above, we contend that the beneficial effect of cosolvent on dissolution kinetics reaches a maximum when the solvent–cosolvent interactions (FC) are nearly balanced by the solvent–polymer interactions (SP). Above a certain cosolvent fraction (e.g., $f_{DCM} = 0.5$), the amount of FA available to interact with both cosolvent and amide groups is reduced, so the rate-limiting step of decrystallization by H-bond breakage is slower despite larger ΔG_{solv} (see H-bond titration results, Figure S3). Figure 4b displays the initial dissolution rates (r_D) of PA6-α in terms of polymer chains (moles) per unit surface area (cm^2) per unit time (sec), as a function of competitive solvation:

$$r_D = f(\Delta G_{solv}) \approx f(\Delta E_{SP} - \Delta E_{FC}) \quad (1)$$

As the cosolvent ratio increases, FA–FA interactions decrease slowly at first while DCM-DCM interactions increase slowly and this trade-off results in an initial increase in FA–DCM interactions until $f_{DCM} = 0.5$, but the FA-FA interactions decrease more rapidly above this point (Table S3), as reflected by the FA carbonyl shift (Figure 3d). Meanwhile, the polyamide solvation energy continues to increase due to favorable vdW. Thus, the quantity ΔE_{SP}–ΔE_{FC} drastically decreases at $f_{DCM} > 0.5$ and corresponds to reduced r_D (and k_m).

Recycling Protocol and Regenerated PA

The unprecedented dissolution kinetics achieved by the present cosolvent strategy can be utilized to establish a room-temperature protocol for dissolution-based recycling of PA-containing waste with an ultra-small carbon footprint. Figure 5a illustrates the general scheme for polyamide-targeted rapid dissolution with photos of some specific conditions for separating and recovering PAs as well as secondary materials (SMs). After precipitating the polymer in acetone (PA6: 99.2% yield), we completely separated and recovered all three solvents by sequential rotary evaporation with high yield (FA: 99.5%, DCM: 98.5%, acetone: 98.2%). The evaporation rate of the cosolvent system is considerably lower than that expected for a linear mixture, suggesting that DCM is stabilized by interactions with FA and thus solvent loss by evaporation is subdued (Figure S9). Residual solvents in recycled PA6 and PA66 after just one washing cycle were examined by headspace gas chromatography (HS-GC) and revealed minor and trace amounts of FA (200–300 ppm) and DCM (1 ppm), respectively (Table S4). There are no universal limits for residual solvent in recycled plastics in general, as different plastic types and applications (e.g., food packaging versus electrical components) all have different purity requirements, but the levels in our study are well below the strict limits set for pharmaceuticals, for example (FA: <5000 ppm, DCM: <600 ppm).[60]

Unlike past research reports and patented technologies,[17,23,24] this formic acid-based cosolvent system does not cause any change in molecular weight or chemical structure such as hydrolysis or oxidation, as shown by GPC, FTIR, and DSC analyses (Figures 5b–d and S10). Conducting the recycling process at lower temperatures also reduces the risk of hydrolysis, since dissolution and degradation coexist with competing temperature-dependent kinetics. Most importantly, no significant changes in mechanical properties were observed, as the unchanged strength, modulus, and elongation can be seen in Figures 5e and S10. The majority of PA dissolution studies from the literature either indicate a decrease in material quality of the range 5%–15% (in terms of M_w or tensile properties) or simply do not report the recycled material's structure/properties.[17–24,61]

Low-Emissions Resource Recovery

We extended the survey to include molding compounds containing various polyamides (PA6, PA66, PA11, PA12,

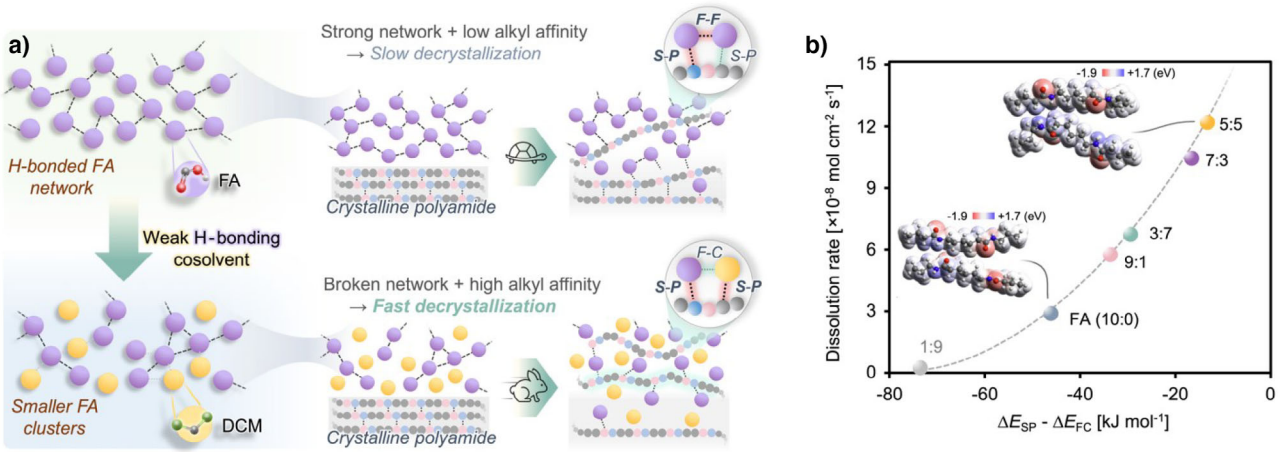

Figure 4. (a) Illustration of proposed mechanism for cosolvent-enhanced dissolution kinetics of polyamide: weak H-bonding solvents break up the strong FA network, increasing solvent-polymer interaction and accelerating the decrystallization process. In pure FA, the solvent-solvent interaction (FF) and solvent-amide interaction (SP) are strong, while the solvent-methylene interaction (SP) is weak. By contrast, DCM regulates the H-bonded solvent network to weaken solvent-solvent interaction (FC) while the SP at both amide and methylene sites are strong. (b) The continuous relationship between the observed dissolution rate (moles of PA chains per unit surface area per unit time) and the difference between solvent-polymer interaction (solvation energy) and solvent-cosolvent interaction.

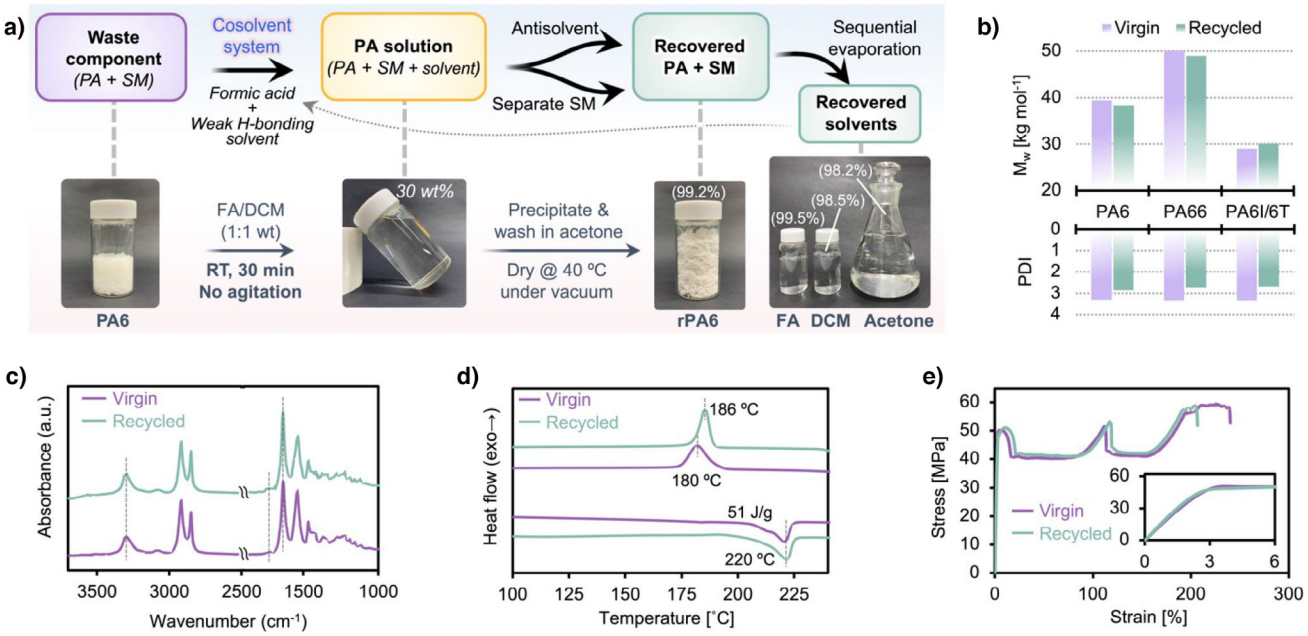

Figure 5. a) Schematic of a dissolution-based recycling protocol with photographs for specific example conditions. Waste components containing PA plastic (with or without secondary materials, SMs) are dissolved in the cosolvent system at room temperature without the need for agitation, yielding a PA solution that can be separated into SMs and PAs prior to precipitation, washing and drying. The difference in boiling points for FA, cosolvent and antisolvent allow them to be fully recovered by sequential evaporation. b) Molecular weight (M_w) and polydispersity index (PDI) of PA6, PA66, and PPA (PA6I/6T) before and after one dissolution/regeneration cycle. c) FTIR spectra, d) DSC scans, and e) tensile stress-strain curves of virgin and regenerated (neat) PA6.

and PA6I/6T) and fillers (CF, GF, fluoromica, and sericite), all of which dissolved within an hour at room temperature without any agitation (Figure 6a). Although PA11 and PA12 have been reported to dissolve in FA/DCM at RT for electrospinning and film casting applications,[30,31] investigation into the dissolution mechanism and kinetics has not been reported and our work is the first demonstration of rapid RT dissolution of semi-aromatic in addition to short- and long-chain polyamides. Note that while the semi-aromatic amorphous PA6I/6T rapidly dissolved (−30 min), fully aromatic PPTA (aramid) was completely undissolved even after several months of immersion (Figure S11). Thus, we concluded that any aliphatic-containing PAs are soluble in this cosolvent system. Although we have focused on PA6 in

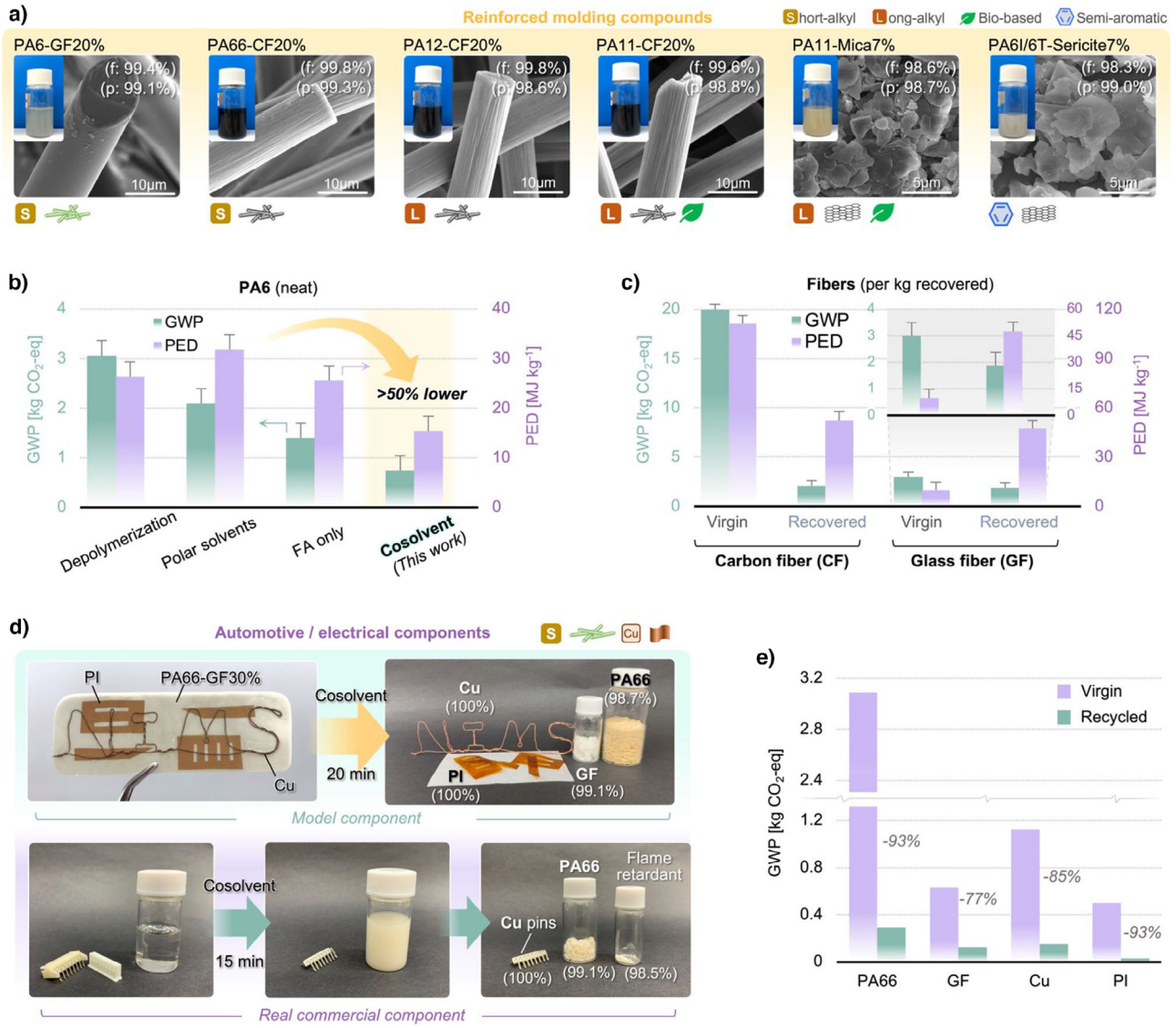

Figure 6. (a) RT dissolution of various PA-based molding compounds: PA6, PA66, PA11, PA12, PA6I/6T, carbon fiber (CF), glass fiber (GF), nanoclay (mica, sericite); symbols indicate the category of composite. Insets are photographs of the solutions (obtained within 30–40 min), and percentages (*f*,*p*) indicate the recovery yield of the filler material and polyamide, respectively. (b) Carbon footprint described by the global warming potential metric (GWP, kg CO_2-eq/kg of material) and primary energy demand (PED, MJ/kg of material) of neat PA6 for different recycling methodologies (Details can be found in the SI). (c) GWP and PED of carbon and glass fibers recovered from PA-based composites; the inset is an enlarged view of GF. Error bars in (b),(c) represent conservative values if solvent recovery efficiency decreases. (d) Application of the cosolvent-based dissolution approach to realistic automotive and electrical components: SMs commonly used together with PA (GF, Cu, PI, flame retardants) were efficiently recovered in pristine condition from model and real components. (e) Comparison of GWPs for each constituent material in their virgin and recovered states.

most of our experiments, we verified the molecular weights of different PAs by GPC and found no significant changes (Figures S10 and S12). The resin and fillers could easily be separated by centrifugation to yield >98% recovery in all cases. SEM observation and WAXD measurements confirm that the resin was fully removed from the fillers and neither the surface nor bulk were chemically damaged throughout the entire process (Figures 6a and S11), since mechanical agitation is not necessary.

We performed a grave-to-gate life cycle analysis (LCA) using the cut-off method[62,63] to investigate the impact of recycling method on global warming potential (GWP) and primary energy demand (PED) associated with reintroducing polyamides into the market, and technoeconomic analysis (TEA) gave the minimum selling price (MSP) needed to break even (see Supporting Information for details). PA6, PA66, and PPAs carry large GWPs (i.e., carbon footprints) and PED of around 6–9 kg CO_2-eq kg^{-1} and 50–60 MJ kg^{-1} for virgin polymer pellets, respectively, which combined with their typical market price ranging from −2.5 \$ kg^{-1} (PA6) up to 15 \$ kg^{-1} (PPAs) translates to high-value resources in terms of embodied carbon and cost.[1,2,6–12] Cutting-edge chemical recycling technology[10] can produce pristine PAs via hydrogenative depolymerization followed by repolymerization via typical condensation reactions, with a grave-to-gate GWP and PED for recycled PA6 (rPA6) about 50% lower than the

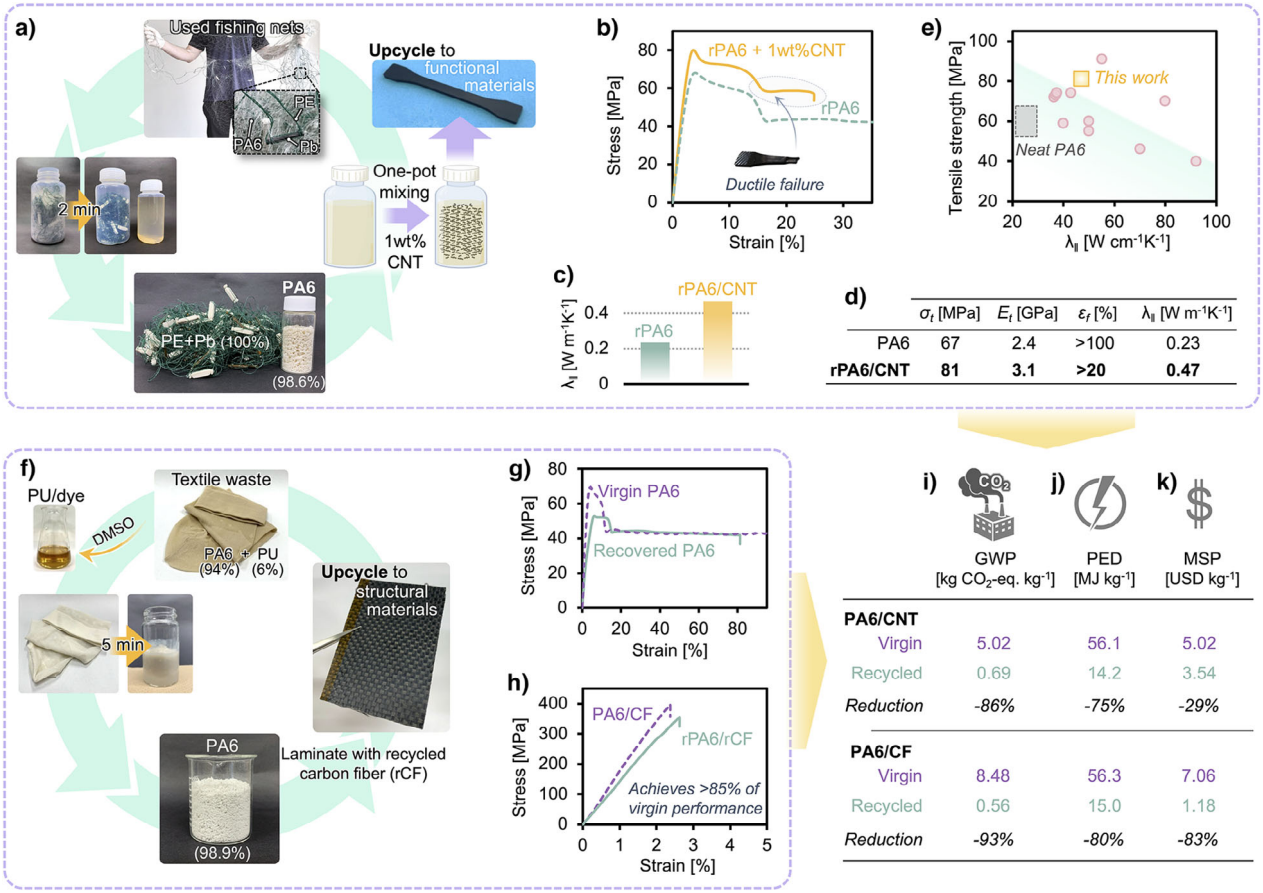

Figure 7. a) Rapid, RT dissolution/separation and fabrication of functional composites: Fishing nets exposed to artificial sea water for 3 months were rapidly dissolved at room-temperature in the cosolvent system and separated to recover PA6, PE, and Pb, followed by dispersion of carbon nanotubes (CNTs) via one-pot solution mixing and injection molding to fabricate rPA6/CNT specimens. b) Tensile behavior and c) thermal conductivity of recycled/upcycled PA6. d) Property summary of recycled/upcycled PA6 materials. e) Multi-functional performance of rPA6/CNT (in terms of strength and thermal conductivity) compared to similar reported composites (see Supporting Information). f) Rapid, RT dissolution/separation and fabrication of structural composites: Waste textiles containing PA6 and polyurethane (removed along with dyes by DMSO) were rapidly dissolved at room-temperature in the cosolvent system and precipitated to recover PA6, followed by lamination with woven carbon fibers previously recycled (rCF) using the cosolvent system. Tensile behavior of g) rPA6 resin and h) rPA6/rCF laminates. Carbon footprint and economic analysis of CF laminates and CNT nanocomposites: i) GWP, j) PED, and k) MSP.

virgin material (Figure 6b and Tables S7–S8). By comparison, conventional dissolution methods using polar solvents[1,24] produce fewer carbon emissions than depolymerization, but energy demand for the high temperatures necessary for dissolution is still considerably large. A hypothetical case of pure FA as solvent reduces the GWP substantially, but the slow dissolution kinetics influences output rate and ultimately results in large energy demand. Our cosolvent strategy for accelerating PA dissolution kinetics at RT without agitation can potentially reduce the GWP of any aliphatic-containing PA down to 0.8 kg CO_2-eq with a PED of just 16 MJ kg^{-1}; this is over 50% lower than depolymerization or conventional dissolution, and roughly 80% lower than virgin material.

Since a variety of SMs can also be recovered in pristine condition, we also considered the recovery of valuable resources such as glass fibers (GF), which are used in high volume, and carbon fibers (CF), which carry a large carbon footprint and high cost (Figure 6c). If our cosolvent-based approach was used to recovery only the fibers (i.e., ignoring the plastic) in model compounds containing 30 wt% short fibers, allocating the full GWP and PED to the fiber fraction alone would still yield drastically reduced emissions compared to virgin fibers.

We further demonstrate this by dissolving PA-based composites as found in automotive and electrical/electronic components (Figures 6d and S13). In addition to PA66, which is rapidly dissolved under ambient conditions, GF, polyimide (PI), and copper were efficiently recovered in pristine condition, and even flame retardant (identified as melamine-cyanurate) were easily separated and recovered in high yield; this attests to the practical merit of the cosolvent system for efficient recycling of realistic composites. The corresponding GWP and PED for each high-value constituent is shown in Figure 6e. In addition, the MSP (i.e., grave-to-gate cost) was calculated as 1.4 \$ kg^{-1} for all types of PA plastic, which is 50% lower than virgin PA6 and 90% lower than virgin PPAs (Table S9). When high-value SMs are produced through the process, the cost is distributed to each constituent and the MSP of PAs and fibers can be reduced to 0.8 and 2.1 \$ kg^{-1}, respectively.

Low-emissions Upcycling of PA Waste

Finally, we extend our approach to upcycle real PA waste into valuable composite materials. Figure 7a shows a facile process in which used fishing nets (containing PA6, PE, and Pb) are rapidly dissolved in the FA/DCM system and separated (see Movie S1), after which carbon nanotubes (CNTs) are mixed into the PA6 to produce functional nanocomposites (Figure S14). The tensile properties and thermal conductivity (Figures 7b–e) are competitive with similar nanocomposites produced using pristine materials as reported in the literature (see Supporting Information for details). Similarly, PA6 was extracted from used textile waste (containing PA6, PU elastomer, and dyes) by first removing the acid dye and elastomer in DMSO before rapidly dissolving the PA in FA/DCM (see Movie S2) and laminating with recycled carbon fiber cloth (rCF) that was previously recovered by dissolution (Figure 7f). The tensile properties of the recovered neat PA (rPA6) were lower than virgin PA6 (Figure 7g), likely to a difference in grades, but the mechanical performance of the rPA6/rCF laminates exceeded 85% of the virgin equivalent and thus could be used in structural applications. LCA/TEA calculations summarized in Figure 7i of the GWP, PED, and MSP of these two upcycled composite materials show reductions of up to 90% compared to similar virgin materials. This demonstrates that rapid, dissolution-based room-temperature recycling processes with minimal carbon emissions can achieve a good balance between material performance, carbon footprint, and cost. Our cosolvent strategy for drastically enhancing RT dissolution kinetics is one promising approach to accomplish this.

Conclusion

Closing the loop for polyamides remains difficult due to the high energy demand and carbon emissions associated with current dissolution-based recycling methods, despite showing great promise for efficient separation of valuable materials in mixed polyamide waste. In this work, we have demonstrated that formic acid, a relatively cheap and environmentally benign solvent known to dissolve short-chain PAs, can be used for rapid, room-temperature recycling of all varieties of PAs when a weak hydrogen-bonding cosolvent is added. Through a combination of experiments and DFT calculations, we showed that: 1) polyamides dissolve when the interactions with H-bonding solvents (having both HBA and HBD characteristics) are more favorable than polymer-polymer interactions, and 2) the cosolvent can tune the solvation behavior of FA toward PA with drastically accelerated dissolution rates by regulating both solvent–solvent and solvent–polymer interactions. While DCM (or another chlorinated solvent) was used as a model cosolvent, the major value of this work is the improved understanding of how cosolvent systems interact with polyamides at the molecular level, providing a foundation for future work on cosolvent design.

Calculations of carbon emissions and energy demand associated with the cosolvent-based recycling process indicate that unprecended performance can be achieved, reaching less than 0.8 kg CO_2-eq kg^{-1} and 15 MJ kg^{-1}, respectively. As formic acid can be directly synthesized from CO_2,[64,65] future developments could see RT recycling processes reduce emissions even further. Besides a stand-alone dissolution-based recycling protocol, this cosolvent strategy can also be applied in intermediate steps in the chemical recycling process in cases where separation using conventional methods is difficult. Further work is needed to find more environmentally-friendly alternative solvents, but we anticipate the findings in this study will guide the design of cosolvent systems for application to other high-value plastics in order to realize resource circularity and carbon neutrality.

Supporting Information

Details regarding experimental and computational methods, as well as supplementary results and LCA/TEA calculations can be found in the Supporting Information.

Acknowledgements

The authors thank M. Kamon (NIMS) for assistance with sample preparation and characterization, DJK Corp. for GPC analysis, Sumika Chemical Analysis Service Ltd. for HS-GC analysis, and K. Naito (NIMS) for access to shared facilities.

Conflict of Interests

The authors declare no conflict of interest.

Data Availability Statement

The data that support the findings of this study are available from the corresponding author upon reasonable request.

Keywords: Carbon Footprint · Cosolvent · Dissolution · Polyamides · Recycling

[1] V. Hirschberg, D. Rodrigue, *J. Polym. Sci.* **2023**, *61*, 1937–1958.
[2] "Global Nylon Market Size, Share & Trends Analysis Report by Product, by Region, and Segment Forecasts, 2021–2028", can be found under: https://www.researchandmarkets.com/reports/4375423/global-nylon-market-size-share-and-trends, 2022 (accessed Jan 20, 2025).
[3] M. Bachmann, C. Zibunas, J. Hartmann, V. Tulus, S. Suh, G. Guillén-Gosálbez, A. Bardow, *Nat. Sustain.* **2023**, *6*, 599–610.
[4] S. R. Nicholson, N. A. Rorrer, A. C. Carpenter, G. T Beckham, *Joule* **2021**, *5*, 673.
[5] M. MacLeod, H. P. H. Arp, M. B. Tekman, A. Jahnke, *Science* **2021**, *373*, 61–65.
[6] R. A. Clark, M. P. Shaver, *Chem. Rev.* **2024**, *124*, 2617–2650.
[7] L. Ye, X. Liu, K. B. Beckett, J. O. Rothbaum, C. Lincoln, L. J. Broadbelt, Y. Kratish, T. J. Marks, *Chem* **2024**, *10*, 172–189.
[8] U. Češarek, D. Pahovnik, E. Žagar, *ACS Sustainable Chem. Eng.* **2020**, *8*, 16274–16282.
[9] A.-J. Minor, R. Goldhahn, L. Rihko-Struckmann, K. Sundmacher, *Chem. Eng. J.* **2023**, *474*, 145333.

[10] A. Kumar, N. von Wolff, M. Rauch, Y.-Q. Zou, G. Shmul, Y. Ben-David, G. Leitus, L. Avram, D. Milstein, *J. Am. Chem. Soc.* **2020**, *142*, 14267–14275.
[11] W. Lv, M. Li, Y. Tao, *Angew. Chem. Int. Ed.* **2024**, *63*, e202402541.
[12] M. Tang, J. Shen, F. Zhang, Y. Zhao, T. Gan, W. Zeng, R. Li, D. Wang, B. Han, Z. Liu, *Angew. Chem. Int. Ed.* **2025**, *64*, e202416436.
[13] P. P. X. Yap, Z. Yen, T. Salim, H. C. A. Lim, C. K. Chung, Y. M. Lam, *Polym. Degrad. Stabil.* **2024**, *225*, 110773.
[14] O. V. Semperger, A. Suplicz,*Sci. Rep.* **2023**, *13*, 17130;
[15] F. Lv, D. Yao, Y. Wang, C. Wang, P. Zhu, Y. Hong, *Compos. Part B* **2015**, *77*, 232–237.
[16] F. G. De Albuquerque Dias, A. G. Veiga, A. P. A. D.a C. P. Gomes, M. L. M. Rocco, M. F. Da Costa, *J. Appl. Polym. Sci.* **2024**, *141*, e55195.
[17] C. D. Papaspyrides, C. N. Kartalis, *Polym. Eng. Sci.* **2000**, *40*, 979–984.
[18] C. N. Kartalis, J. G. Poulakis, C. J. Tsenoglou, C. D. Papaspyrides, *J. Appl. Polym. Sci.* **2002**, *86*, 1924–1930.
[19] M. A. R. Önal, S. Dewilde, M. Degri, L. Pickering, B. Saje, S. Riaño, A. Walton, K. Binnemans, *Green Chem.* **2020**, *22*, 2821–2830.
[20] Y.-B. Zhao, X.-D. Lv, H.-G. Ni, *Chemosphere* **2018**, *209*, 707–720.
[21] M. Klotz, C. Oberschelp, C. Salah, L. Subal, S. Hellweg, *Sci. Tot. Environ.* **2024**, *906*, 167586.
[22] S. R. Chandrasekaran, S. Avasarala, D. Murali, N. Rajagopalan, B. K. Sharma, *ACS Sustainable Chem. Eng.* **2018**, *6*, 4594–4602.
[23] A. Maeurer, M. Schlummer, O. Beck, (Fraunhofer-Gesellschaft), US Patent 8138232B2, **2008**.
[24] F. Knappich, M. Klotz, M. Schlummer, J. Wölling, A. Mäurer, *Waste Manage.* **2019**, *85*, 73–81.
[25] T. W. Walker, N. Frelka, Z. Shen, A. K. Chew, J. Banick, S. Grey, M. S. Kim, J. A. Dumesic, R. C. Van Lehn, G. W. Huber, *Sci. Adv.* **2020**, *6*, eaba7599.
[26] K. L. Sánchez-Rivera, P. Zhou, M. S. Kim, L. D. González Chávez, S. Grey, K. Nelson, S.-C. Wang, I. Hermans, V. M. Zavala, R. C. Van Lehn, G. W. Huber, *ChemSusChem* **2021**, *14*, 4317–4329.
[27] C. M. Hansen, *Hansen Solubility Parameters: A User's Handbook*. CRC Press, Boca Raton, US, **1999**.
[28] M. Bursch, J.-M. Mewes, A. Hansen, S. Grimme, *Angew. Chem.* **2022**, *134*, 202205735.
[29] A. V. Marenich, C. J. Cramer, D. G. Truhlar, *J. Phys. Chem. B* **2009**, *113*, 6378–6396.
[30] K. Behler, M. Havel, Y. Gogotsi, *Polymer* **2007**, *48*, 6617–6621.
[31] T. Wen, Y. Gao, J. Zhou, J. Qiu, S. Wang, J. Loos, D. Wang, X. Dong, *ACS Macro Lett.* **2023**, *12*, 697–702.
[32] S. Anwar, D. Pinkal, W. Zajaczkowski, P. von Tiedemann, H. S. Dehsari, M. Kumar, T. Lenz, U. Kemmer-Jonas, W. Pisula, M. Wagner, R. Graf, H. Frey, K. Asadi, *Sci Adv.* **2019**, *5*, eaav3489.
[33] A. J. Ragauskas, G. W. Huber, J. Wang, A. Guss, H. M. O'neill, C. S. K.i Lin, Y. Wang, F. R. Wurm, X. Meng, *ChemSusChem* **2021**, *14*, 3982–3984.
[34] H. Li, H. A. Aguirre-Villegas, R. D. Allen, X. Bai, C. H. Benson, G. T. Beckham, S. L. Bradshaw, J. L. Brown, R. C. Brown, V. S. Cecon, J. B. Curley, G. W. Curtzwiler, S. Dong, S. Gaddameedi, J. E. García, I. Hermans, M. S. Kim, J. Ma, L. O. Mark, M. Mavrikakis, O. O. Olafasakin, T. A. Osswald, K. G. Papanikolaou, H. Radhakrishnan, M. A. Sanchez Castillo, K. L. Sánchez-Rivera, K. N. Tumu, R. C. Van Lehn, K. L. Vorst, M. M. Wright, et al., *Green Chem.* **2022**, *24*, 8899–9002.
[35] *Nat. Sustain.* **2023**, *6*, 1137.
[36] X. Mu, Q. Wang, L.-P. Wang, S. D. Fried, J.-P. Piquemal, K. N. Dalby, P. Ren, *J. Phys. Chem. B* **2014**, *118*, 6456–6465.
[37] F. Caporaletti, L. Gunkel, M. Á.n. Fernández-Ibáñez, J. Hunger, S. Woutersen, *Angew. Chem. Int. Ed.* **2024**, *63*, e202416091.
[38] W. Nernst, *J. Physik. Chem.* **1904**, *47*, 4704.
[39] R. J. Seager, A. J. Acevedo, F. Spill, M. H. Zaman, *Sci. Rep.* **2018**, *8*, 7711.
[40] Y. Zhao, D. G. Truhlar, *Theor. Chem. Acc.* **2008**, *120*, 215–241.
[41] F. Weigend, *Phys. Chem. Chem. Phys.* **2006**, *8*, 1057.
[42] A. E. Meyer, J. A. Davies, A. M. Ellis, *Phys. Chem. Chem. Phys.* **2020**, *22*, 9637–9646.
[43] E. M. S. Maçôas, J. Lundell, M. Pettersson, L. Khriachtchev, R. Fausto, M. Räsänen, *J. Mol. Spectrosc.* **2003**, *219*, 70–80.
[44] A. Olbert-Majkut, J. Ahokas, J. Lundell, M. Pettersson, *Chem. Phys. Lett.* **2009**, *468*, 176–183.
[45] R. da Silva Alvim, A. E. Bresciani, R. M. B. Alves, *J. Mol. Model.* **2024**, *30*, 67.
[46] S. Lopes, R. Fausto, L. Khriachtchev, *Mol. Phys.* **2019**, *117*, 1708–1718.
[47] Y. Han, Z. Wang, R. Qiao, J. Cheng, C. Jiang, H. Wang, *Phys. Chem. Chem. Phys.* **2023**, *25*, 18048–18055.
[48] S.-L. Chen, D.-X. Zhao, L.-D. Gong, Z.-Z. Yang, *Theor. Chem. Acc.* **2010**, *127*, 627–639.
[49] X. Pang, W. J. Jin, *New J. Chem.* **2015**, *39*, 5477–5483.
[50] A. Mukhopadhyay, M. Mukherjee, P. Pandey, A. K. Samanta, B. Bandyopadhyay, T. Chakraborty, *J. Phys. Chem. A* **2009**, *113*, 3078–3087.
[51] L. Almásy, A. Bende, *Molecules* **2019**, *24*, 1810.
[52] O. Persyn, V. Miri, J. M. Lefebvre, C. Depecker, C. Gors, A. Stroeks, *Polym. Eng. Sci.* **2004**, *44*, 261–271.
[53] D. Galimberti, C. Quarti, A. Milani, L. Brambilla, B. Civalleri, C. Castiglioni, *Vibrat Spectrosc.* **2013**, *66*, 83.
[54] Y. Ma, T. Zhou, G. Su, Y. Li, A. Zhang, *RSC Adv.* **2016**, *6*, 87405–87415.
[55] D. S. Boucher, *J. Appl. Polym. Sci.* **2020**, *137*, 48908.
[56] B. A. Miller-Chou, J. L. Koenig, *Prog. Polym. Sci.* **2003**, *28*, 1223–1270.
[57] D. A. Sverjensky, *Nature* **1992**, *358*, 310–313.
[58] P. Martin, J. J. Gaitero, J. S. Dolado, H. Manzano, *ACS Earth Space Chem. 2021* **2021**, *5*, 516–524.
[59] A. Zupanc, J. Install, T. Weckman, M. M. Melander, M. J. Heikkilä, M. Kemell, K. Honkala, T. Repo, *Angew. Chem. Int. Ed.* **2024**, *63*, e202407147.
[60] I. C. H. Expert Working Group, Impurities: Guidelines for Residual Solvents (International Council for Harmonisation of Technical Requirements for Pharmaceuticals for Human Use)**2021**, Q3C-R8.
[61] M. Hattori, M. Saito, K. Okajima, K. Kamide, *Polym J* **1995**, *27*, 631–644.
[62] T. Ekvall, G. S. Albertsson, K. Jelse, *Modeling recycling in life cycle assessment* (IVL Swedish Environmental Research Institute), Gothenburg, Sweden, Project No. 4720–1, **2018**.
[63] S. L. Nordahl, C. D. Scown, *Chem. Sci.* **2024**, *15*, 9397–9407.
[64] C. Zhang, X. Hao, J. Wang, X. Ding, Y. Zhong, Y. Jiang, M.-C. Wu, R. Long, W. Gong, C. Liang, W. Cai, J. Low, Y. Xiong, *Angew. Chem. Int. Ed.* **2024**, *63*, e202317628.
[65] S. Kibria Nabil, S. Mccoy, M.d G. Kibria, *Green Chem.* **2021**, *23*, 867–880.

Manuscript received: January 29, 2025
Revised manuscript received: April 29, 2025
Accepted manuscript online: May 21, 2025
Version of record online: June 05, 2025